

DESIGN STUDIES ON NLF AND HLFC APPLICATIONS AT DLR

Arne Seitz, Karl-Heinz Horstmann
DLR – Institute of Aerodynamics and Flow Control

Keywords: *natural laminar flow; hybrid laminar flow control; wing design; drag reduction*

Abstract

The Vision 2020 of the Advisory Council for Aeronautical Research in Europe (ACARE) demands an environmentally friendly and sustainable growth of air transport. The goal is to substantially reduce emissions of carbon dioxides (by 50%) and nitrogen oxides (by 80%). But also lowering costs (by 30%) plays an important role.

It is obvious that such ambitious goals cannot be matched with small improvements on existing aircraft designs but are only possible with a leap in technology. In the field of aerodynamics boundary laminarization offers such a leap because of its high potential in drag and, hence, fuel burn reduction.

At the German Aerospace Center DLR research on laminar flow for transport aircraft flying in the transonic regime started by the mid eighties of the last century. Basic as well as applied research was performed. The intention of the present paper is to give an overview on design studies for transonic wings with natural laminar flow (NLF) and hybrid laminar flow control (HLFC) performed at DLR over a period of 25 years. Design principals and the tools used are explained.

1 Introduction

The demand to reduce emissions considerably but also increasing costs enforces new aircraft designs with drastically improved fuel efficiency. It is well known that aerodynamics can play a major role to achieve this goal by employing the knowledge about laminar-turbulent transition and its control: Extensive laminar boundary layer flow will reduce friction and

friction induced pressure drag on wetted surfaces of an aircraft considerably.

Consequently, the systematic design of so-called laminar airfoils started already around 1940, [1], [2]. Today, laminar airfoils are widespread used in sailplane and light aircraft designs [3], [4], but practically all applications of laminar flow technology put into operation are more or less restricted to straight wings flying at moderate Reynolds and Mach numbers. For the designer this is the easier case to treat because he has to cope with only one transition phenomenon, namely Tollmien-Schlichting instability (TSI).

The situation becomes more complicated for transonic swept wings. Here at least two more transition phenomena come into effect, namely attachment line instability (ALI) and crossflow instability (CFI).

For moderate sweep angles and Reynolds numbers extensive laminar flow can still be achieved by natural means (NLF), i.e. solely by contour shaping of the airfoil sections. On larger transport aircraft flying at higher speeds, the combination of sweep and Reynolds number requires additional active flow control measures like suction to enhance the stability of the laminar boundary layer leading to the hybrid laminar flow concept (HLFC).

Basic research on the different transition phenomena has been conducted over decades (e.g. [5], [6], [7], [8], [9], [10], [11], [12]) leading to a good knowledge about the principle flow physics and how to control them. In the following paragraphs it will be explained how at DLR this knowledge base was utilized to build up the capability to design transonic laminar wings following the NLF and HLFC concepts.

2 Basic Principles of Laminar Wing Design

2.1 Transition Prediction

The most important tool needed for the design of a laminar flow wing is a fast and reliable transition prediction method. A lot of different approaches to this problem exist. At DLR the semi-empirical e^n method, established by van Ingen [13], is utilized.

The e^n method is based on linear stability theory. The velocity profiles of the laminar boundary layer are analyzed with respect to their stability against harmonic oscillations which are superimposed as small disturbances. If unstable, the downstream amplitude growth of a disturbance can be expressed by the so called n -factor. It is defined as the natural logarithm of the ratio of disturbance amplitude at a point downstream to its initial values. It is assumed that transition (or, respectively, onset of turbulence) occurs where the n -factor of the most amplified disturbance reaches a limiting value n_{crit} .

Boundary layer velocity profiles on a swept wing in regions where a pressure gradient is present are three-dimensionally warped. When projecting them into the direction of the edge flow, one will find a velocity profile that is very similar to those of two-dimensional boundary layers, while in a direction perpendicular to that a so called crossflow profile exists. As it is known from 2d flow cases, the profiles in direction of the edge flow can become unstable against small travelling disturbances, i.e. Tollmien-Schlichting waves, while the crossflow profiles exhibit at least one inflectional point making them inherently unstable against disturbances with a wave vector approximately pointing in crossflow direction.

Consequently, in the approach followed at DLR [14] for transition prediction due to TSI and CFI, chordwise n -factor distributions for two classes of disturbances are calculated:

1. Tollmien-Schlichting instabilities are treated as travelling waves with a propagation direction specified to be always tangential to the flow at the boundary layer edge.

2. Crossflow instabilities are treated as stationary (zero frequency) waves.

In order to obtain values of n_{crit} for TSI and CFI, well defined experiments have to be performed. Based on measured pressure distributions boundary layer velocity profiles are calculated and subsequently analyzed with respect to their stability. In a third step, the envelopes of n_{TS} and n_{CF} distributions are correlated with the measured transition locations from the same experiment.

For the design studies presented here the transition criterion evaluated from the ATTAS flight experiments [15], [16] performed in 1987 was employed, Fig.1. Here, a wing glove on a transport aircraft was designed especially for the purpose of an easy n -factor correlation. The validity of the criterion found was successfully demonstrated during design and flight testing of a NLF glove on a Fokker 100 in 1991 [17]. In contrast to the ATTAS flight tests, the main goal here was to assess the performance gain of a NLF wing design.

It is believed that the ATTAS criterion, although evaluated on a NLF glove, is also valid for HLFC applications, provided suction rates are small and do not introduce additional strong disturbances into the laminar boundary layer (in praxis an ideal suction surface cannot be realized; suction through slits or holes is, up to a certain degree, always inhomogeneous).

Of course, during the wing design process not only TSI and CFI must be controlled by an appropriate shaping of airfoil sections and, in case of HLFC, suction distribution. As mentioned above, transition may already occur at the attachment line. In our design process we check for attachment line transition, ALT, following the ideas of Pfenninger [8]. He pointed out that a Reynolds number based on the momentum loss thickness at the attachment line, Re_θ , should be an appropriate parameter for defining the state of the boundary layer flow: if viscous forces acting on fluid elements dominate inertia forces, i.e. Re_θ remains low, the formation of turbulent eddies at the attachment line will be suppressed, even in the presence of large disturbances coming for example from the turbulent boundary layer of the fuselage. By evaluation of different experiments, Pfenninger

specified a critical value of $Re_\theta = 100$ as transition criterion, which is also used in our wing design procedure. The actual value of Re_θ can be computed by

$$Re_\theta = \theta^* \sin \Phi_{LE} \sqrt{Re_c / (du/ds)} \quad (1)$$

Herein Φ_{LE} is the wing leading edge, Re_c the local chord Reynolds number and du/ds the flow acceleration at the attachment line. The factor θ^* equals 0.404, but can be reduced by applying suction according to a functional dependency suggested by Pfenninger [8].

In principle the Pfenninger criterion for ALT was confirmed by the ATTAS flight tests for NLF applications but for cases with boundary layer suction at the attachment line still some uncertainty exists. However, Schrauf suggests a criterion derived from an evaluation of the A320 hybrid laminar fin flight experiment [18], which is based on Polls investigations on ALT, [9].

It should be noted that the transition criteria described above are valid for flight in free atmosphere. Experience gained so far shows that for wind tunnels, due to the different disturbance environment, the limiting n-factors for TSI and CFI can deviate considerably. Of course this can have an impact on performance tests for laminar wing designs intended for free flight conditions. Therefore it is necessary to qualify each wind tunnel for laminar flow experiments through an individual n-factor correlation. For the European transonic wind tunnel (ETW) this has been done within the frame of the EU funded project TELFONA, [19].

2.2 Target Pressure Distributions

In parametric studies performed at DLR [20] in the mid 1980's the characteristics of pressure distributions which can prevent early transition induced by one of the aforementioned mechanisms ALT, CFI and TSI were worked out. At the design point, the section pressure distributions of a transonic swept wing should be tailored to allow for

- an extent of laminar flow as high as possible,

- laminar flow for a certain range of lift coefficients ΔC_L and
- low wave drag (i.e. recompression on the upper side with a weak shock), even in off design.

Fig. 2 shows a typical target pressure distribution matching these demands. According to the transition criterion for ALT, a steep gradient du/ds , which means strong flow acceleration in the attachment line region, minimizes Re_θ and thus is a means to avoid ALT.

The growth of CFI is triggered by the intensity of the boundary layer crossflow velocity profile, which in turn is related to the pressure gradient of the outer flow. Therefore, on a swept wing, it would be desirable to have everywhere constant pressure without any gradients. Of course, this is not possible, since some lift has to be produced and, hence, a pressure gradient has to be specified to pass over from the attachment line pressure to the selected levels on upper and lower side of the airfoil.

The idea we follow to prevent early transition due to CFI is to maintain the initial strong flow acceleration in the nose region and then to change over from the steep pressure gradient to a moderate one quite sharply. Because the boundary layer still is very thin and viscous forces dominate, the growth of unstable (short wavelength) crossflow disturbances in the front acceleration zone will not reach a dangerous size, provided their amplification is cut off immediately by easing down the crossflow intensity when reaching the desired pressure level.

The latter measure can be supported by a small suction peak. Behind the suction peak, the adverse pressure gradient will turn the direction of the boundary layer crossflow velocity profile shortly and, hence, changes the sign of vorticity in the basic flow. This will suppress stationary crossflow vortices, formed in the front acceleration zone.

However, the sharpness or roundness, respectively, of the change over can be chosen dependent on the actual chord Reynolds number ("the higher the sharper") and if suction will be applied or not ("if suction, then round").

As it is well known from two-dimensional boundary layers, the growth of TSI can be limited by a favourable pressure gradient. This gra-

dient might increase with increasing boundary layer thickness, i.e. increasing local Reynolds number, leading to a slightly concave shape of the pressure distribution. Nevertheless, any pressure gradient will promote the amplification of CFI. Therefore a good compromise has to be found to fulfil at the same time the requirements for prevention of transition due to CFI and TSI over the mid chord region. This compromise is influenced by the chord Reynolds number of the special design case.

Of course, when ALT, CFI and TSI have successfully been avoided, the pressure minimum and pressure recovery on the upper side of the wing section should be chosen in order to obtain a recompression with a shock and, hence, wave drag, as weak as possible. The aft recompression zone of upper and lower side can be designed conventionally, for example in order to match lift requirements by introducing rear loading.

Beneath the pressure distribution, chord Reynolds number and sweep angle are further important parameters influencing boundary layer stability characteristics: For a given pressure distribution, transition moves forward with increasing values of any of both parameters. So conditions may arise, under which laminar flow is no longer achievable solely by the natural means of tailoring pressure distributions respectively contour shaping. In this case boundary layer suction is available as another powerful means for the controlling of stability characteristics. But it is obvious, that in the interest of minimization of suction power and simplicity of the suction system the rules for target pressure distributions given above should be applied not only in a NLF design but also in the case of a HLFC wing.

Furthermore it should be noted that laminar flow at high Reynolds numbers and sweep angles is very sensitive to deviations from the ideal section pressure distributions. Therefore it is not sufficient to simply design airfoil sections good for laminar flow on an infinite swept wing and use these as generators for a 3d wing. In fact, it is necessary to resolve as far as possible by the computational methods used all three-dimensional (finite wing, centre effect) as well as interference effects (wing-body, wing-engine

nacelle) and modify wing profiles until section pressure distributions match the requirements for laminar flow.

3 Laminar Wing Design Studies

In the following paragraphs examples of laminar wing design studies following the NLF and HLFC concept are presented. These studies have been performed throughout the last two decades illustrating the progress that has been made with respect to design capabilities. It should be noted that this list is not exhaustive.

3.1 NLF Applications

With the availability of the transition criterion from the ATTAS flight tests in 1989, a feasibility study on the design of a NLF wing for an A320 type of aircraft was performed at DLR. Here the goal was to work out the principal advantages (viscous drag reduction) and disadvantages of a NLF wing. The design point was chosen to be that of the A320, i.e. $Ma = 0.78$ and $C_L = 0.5$ at a flight level of 11 000m.

It soon turned out that with gradients du/ds achievable at the attachment line and a typical leading edge sweep of a conventional wing ALT will inevitably occur at the expected chord Reynolds numbers. As a consequence, the leading edge sweep was reduced to 19.04° . Furthermore, for simplification, a mono-trapezoidal plan form with a taper ratio of 0.305 was chosen. However, aspect ratio and area were taken the same as for the A320 in order to make results of viscous drag assessments comparable with the baseline aircraft.

Flowfield calculations were performed for a wing-body configuration utilizing an Euler code coupled to a 3d integral boundary layer method. In order to obtain the final design, five generator airfoil sections were iteratively modified (using a 2d inverse panel method) followed by an aerodynamic analysis of the complete configuration until the target pressure distributions were matched, Fig. 3.

As depicted in Fig. 4 the final design fulfills the criterion for ALT along the whole wing span. Fig.5 then shows the result of a section wise determination of n_{TS} and n_{CF} distributions,

delivering the extent of laminar flow on the wing's upper and lower surfaces.

An aerodynamic analysis with the same computational methods was performed for the baseline A320. A drag breakdown for both, NLF and baseline wing, than showed at the design point a reduction of wing friction, wave and pressure drag of 39% which is equivalent to a total drag reduction of 10.4%.

As a second example the design of a NLF wing for a very light jet (VLJ) business aircraft is presented. This work has been conducted within the frame of the EU project CESAR (Cost Effective Small Aircraft), which ended in February 2006. The overall configuration as well as top level aircraft requirements and wing design objectives were defined by Piaggio Aero. The goal then was to design a NLF wing with 20° leading edge sweep for three distinctive cruise conditions (see Tab. 1). Further requirements affected pitching moment coefficient, buffet onset and drag rise as well as some geometrical constraints.

Fig. 7 shows pressure distributions of the final wing at the selected design point. Again, the wing is build up from four generator sections that were iteratively modified to meet the laminar flow requirements. However, in this case the inverse capabilities of the DLR FLOWer code [21] were utilized. For prescribed wing target pressure distributions the code will find the corresponding geometry while incorporating all major 3d and interference effects of the configuration under consideration (here: wing-body-engine).

However, the final aerodynamic analysis of the VLJ configuration was done employing the DLR Tau code [22], which features an automatic transition prediction module [23] on basis of the principles described in paragraph 2.1.

In Fig. 7 iso-surfaces of the skin friction coefficient c_f are presented for the design point. Low c_f values can be identified on upper and lower side of the wing corresponding with those areas wetted by laminar flow.

Fig. 8 then shows the most important information with respect to the assessment of the design: Lift curve, pitching moment and drag polar for cruise priority 1 - 3. It can be seen that for almost the whole range of operational lift

coefficient a benefit in the order of 32 drag counts from laminar flow can be expected. Furthermore, the required maximum lift coefficient $C_{L,max}$ in all cruise conditions is reached free from buffeting. Finally, drag rise at $C_L = 0.34$ was evaluated, showing that the respective requirement is fulfilled, Fig. 9.

3.2 HLFC Applications

At the same time the NLF design was performed (see paragraph 3.1), a HLFC study was started in 1989. The Outcome of this study revealed that laminarization of the upper side of a wing contributes roughly 2/3 to the viscous drag reduction while only 1/3 originates from the lower side. Furthermore a comparison between contours of profiles designed for the HLFC wing and the baseline A320 wing showed only small deviations on the upper side. These facts gave the motivation to investigate in a follow up study more deeply the feasibility of an upper surface laminar glove for the existing A320 wing outboard of the engine respectively the trailing edge kink. At that time (1993) it was intended to use the study as basis for a technology demonstrator.

Of course, several constraints were imposed on the design, concerning geometrical as well as aerodynamic compatibility: No contour modifications were allowed on the lower side of the wing except in front of the wing box, where also the upper side was free for a completely new shaping. In order to keep the integrity of wing box unaffected the new contour was required to be thicker than the original one in this region. Again, no contour modifications were allowed on the upper side behind the wing box, where spoilers, flaps and aileron are located. Furthermore, in order to minimize changes in lateral stability, the nose down pitching moment of the laminar sections should not differ too much from the original ones.

During the design process, all calculations were performed for a wing-body-pylon-engine configuration. In Fig 10 .the resulting wing pressure distributions are shown for the design point ($Ma = 0.78$, $C_L = 0.4$, $Re_{AMC} = 24.7 \cdot 10^6$), which clearly follow the rules given in paragraph 2.2. Evaluation of transition locations

then delivers the area wetted by laminar flow. Of course, boundary layer suction is applied to achieve this result, especially to reduce n_{cf} to a subcritical value, Fig. 11. Nevertheless, the necessary mass flow rates, Fig. 12, are rather low as is the required power for a pump (approx. 3KW per wing half).

Prediction of power requirements is quite delicate and for the study shown here it is just a rough estimation based on rules of thumb. A detailed systems layout that allows for a fair balancing of aerodynamic benefits against power and weight penalties was not performed.

Therefore, within the EU funded ALTTA (Application of Hybrid Laminar Flow Technology on Transport Aircraft) project [25] the principle architecture as well as an integrated design and analysis procedure of a simple but very effective suction system was elaborated. In Fig. 13 the basic idea is schematically shown for a fin: The outer porous surface, the supporting stringers and the inner sheet form a double sheet surface with a relatively high number of chambers, see Fig. 1. This structure opens a very efficient way to control the suction speed distribution. With the porosity of the suction surface constant in chord and span direction as usual, the local mass flow between two stringers can be adjusted by metering orifices and allow to use the whole L/E box as a single suction duct.

Input for the layout of the system are the required suction mass flow rates from the aerodynamic design but also models for the pressure drop across the porous outer surface and the metering orifices. Especially a correct modelling of the pressure drop relations of these both elements is crucial for a successful layout and, hence, application of a suction system. Therefore, at DLR a “Flowmeter” was designed, Fig. 14, in order to measure the pressure drop as a function of mass flow rates for different test articles under realistic conditions with respect to outside pressure and temperature.

4 Concluding Remarks

Although the principles of transonic laminar wing design have not changed, aerodynamic design and analysis capabilities have improved considerably over the past two decades. This is

mainly due to the fact that CFD method become constantly more and more sophisticated. Today, reliable automatic transition prediction based on linear stability theory for wings and even fuselages is available. Furthermore, modern grid generation procedures allow for a fast and accurate modeling of highly complex configurations leading to an accurate resolution of any interference effect that might have an influence on the extent of laminar flow. So, from a pure aerodynamics point of view a successful application of laminar wing designs can be guaranteed.

Nevertheless wing design has to take into account also structural aspects as well as manufacturing technologies. Therefore, at DLR the multidisciplinary project LamAiR was started, which consists of two technology streams.

The first deals with the design of a forward swept NLF wing for a new short range aircraft. A structural concept based on composite materials that allows for aeroelastic tailoring will be investigated. Of course, fluid-structure coupling then is a crucial issue from the very beginning of the design process. Furthermore, the manufacturing process of panels from composite material will be studied in order to minimize the so called “spring in” that leads to a contour waviness which might have an impact on laminar flow.

The second technology stream is dedicated to HLFC. Beneath an aerodynamic design of a laminar fin the work will comprise investigations on structural concepts for a nose box with integrated suction system as well as the development of manufacturing technologies for porous surfaces of different materials.

References

- [1] Abbot I H, von Doenhoff A H. *Theory of wing sections*. Dover Publications, Inc., New York, 1959
- [2] Doetsch H. Untersuchungen an einigen Profilen mit geringem Widerstand im Bereich kleiner ca-Werte. *Jahrbuch der deutschen Luftfahrtforschung* 1940, pp. I.54-I.57
- [3] Eppler R. *Airfoil design and data*. Springer-Verlag, Berlin / Heidelberg, 1990
- [4] Althaus D, Wortmann F X. *Stuttgarter Profilkatalog I*. Verlag Friedrich Vieweg & Sohn, Braunschweig, 1996

- [5] Tollmien W. Über die Entstehung der Turbulenz. *Nachr. Ges. Wiss. Göttingen, Math. Phys. Klasse*, pp. 21-44, 1929
- [6] Schlichting H. Zur Entstehung der Turbulenz bei der Plattenströmung. *Nachr. Ges. Wiss. Göttingen, Math. Phys. Klasse*, pp. 21-44, 1929
- [7] Pfenninger W. Some Results from the X21 Program. Part I: Flow Phenomena at the Leading Edge of Swept Wings. Recent Developments in Boundary Layer Research. *Part IV. AGARDograp 97*, May 1965.
- [8] Pfenninger W. Laminar Flow Control, Laminarization. *Special course on concepts for drag reduction*, AGARD Report No. 654, 1977
- [9] Poll, D I A. Some aspects of the flow near a swept attachment line with particular reference to boundary layer transition. *Cranfield Inst. of Techn. COA Report No. 7805*, 1978
- [10] Gregory N, Stuart J T, Walker W S. On the stability of three-dimensional boundary layers with application to the flow due to a rotating disk. *Phil. Trans. Roy. Soc. London*, a248, 1952
- [11] Dagenhardt J R. Amplified crossflow disturbances in the laminar boundary layer on swept wing with suction. *NASA TP 1902*, 1982
- [12] Arnal D, Coustols E, Juillen J C. Experimental and theoretical study of transition phenomena on an infinite swept wing. *Recherche Aerospatiale* No. 1984-4, pp. 39-54, 1984
- [13] van Ingen J L. A suggested semi-empirical method for the calculation of the boundary layer transition region. *Report V.T.H. 74*, Aero. Lab. Technische Hochschule Delft, 1956
- [14] Redeker G, Horstmann K-H. Die Stabilitätsanalyse als Hilfsmittel beim Entwurf von Laminarprofilen. *DGLR-Bericht 86-03*, pp. 317-348, 1986
- [15] Redeker G, Horstmann K-H, Koester H, Thiede P, Szodruch J. Design of a Natural Laminar Flow Glove on a Transport Aircraft. AIAA Paper 90-3043, 1990
- [16] Redeker G, Horstmann K-H, Quast A, Dressler U, Bieler H. Flight Tests with a Natural Laminar Flow Glove on a Transport Aircraft. AIAA Paper 90-3044, 1990
- [17] Voogt N. Flight Testing of a Fokker 100 Aircraft with Laminar Flow Glove on a Transport Aircraft. *Proceedings of the second European Forum on Laminar Flow Technology, AAAF Rept.*, AAAF, Paris, pp. 2-3 – 2-14, 1996
- [18] Schrauf G. Evaluation of the A320 hybrid laminar fin experiment. *European Congress on Computational Methods in Applied Sciences and Engineering EC-COMAS 2000*, Barcelona, September 2000
- [19] Schrauf G, Horstman K-H, Streit T, Perraud J, Donelli R. The TELFONA pathfinder wing fort he calibration of the ETW wind tunnel. *KATnet II Conference on Key Aerodynamic Technologies*, Bremen, 2009
- [20] Redeker G, Horstmann K-H, Koester H, Quast A. Laminarprofile fuer Verkehrsflugzeuge. DLR IB-129-86/12, 1985
- [21] Kroll N, Rossow C-C, Becker K, Thiele F. The MEGAFLOW Project. *Aerospace Science and Technology*, Vol. 4, pp. 223-237, 2002
- [22] Schwammborn D, Gerhold, T, Heinrich R. The DLR TAU-Code: Recent Applications in Research and Industry. *Proceedings of the European Conference on Computational Fluid Dynamics (ECCOMAS CFD 2006)*, Delft, The Netherlands, 5. – 8. September 2006
- [23] Krumbein A, Krimmelbein N, Schrauf G. Automatic Transition Prediction in a Hybrid Flow Solver – Part 1: Methodology and Sensitivities. *Journal of Aircraft*, Vol. 46, No. 4, pp. 1176 – 1190, 2009
- [24] Krumbein A, Krimmelbein N, Schrauf G. Automatic Transition Prediction in a Hybrid Flow Solver – Part 2: Practical Application. *Journal of Aircraft*, Vol. 46, No. 4, pp. 1191 – 1199, 2009
- [25] Schrauf G. ALTTA Synthesis Report. Published by the EU under contract N° G4RD-CT2000-00143, project proposal N°GRD1-1999-11192, 2003

Contact Author Email Address

arne.seitz@dlr.de

Copyright Statement

The authors confirm that they, and/or their company or organization, hold copyright on all of the original material included in this paper. The authors also confirm that they have obtained permission, from the copyright holder of any third party material included in this paper, to publish it as part of their paper. The authors confirm that they give permission, or have obtained permission from the copyright holder of this paper, for the publication and distribution of this paper as part of the ICAS2010 proceedings or as individual off-prints from the proceedings.

Tables

| Aerodynamic design objectives at clean aircraft operating points | | | | | |
|--|-----------|-------|-------------------------|------------------|------------------|
| Flight condition | Alt. [ft] | Mach | Re_c root / tip | C_L range wing | $C_{L,max}$ wing |
| Cruise Prio. 1 | 35,000 | 0.694 | 12.3 / $4.6 \cdot 10^6$ | 0.20 – 0.29 | 0.44 |
| Cruise Prio. 2 | 31,000 | 0.716 | 14.6 / $5.4 \cdot 10^6$ | 0.16 – 0.23 | 0.35 |
| Cruise Prio. 3 | 41,000 | 0.610 | 8.2 / $3.1 \cdot 10^6$ | 0.34 – 0.50 | 0.75 |

Table 1. Aerodynamic design objectives for a VLJ business aircraft

Figures

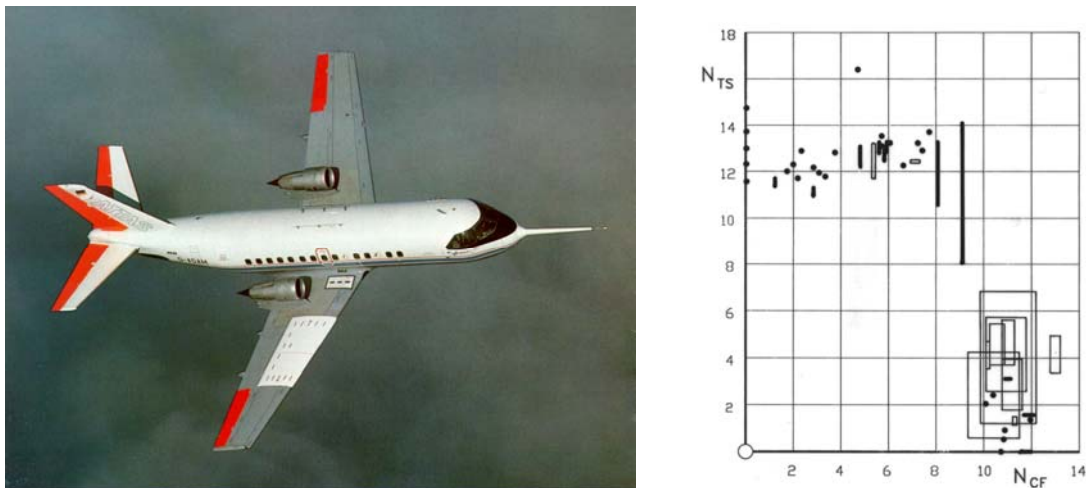


Fig.1. The ATTAS flight experiment and evaluation of the n_{TS} - n_{CF} transition criterion

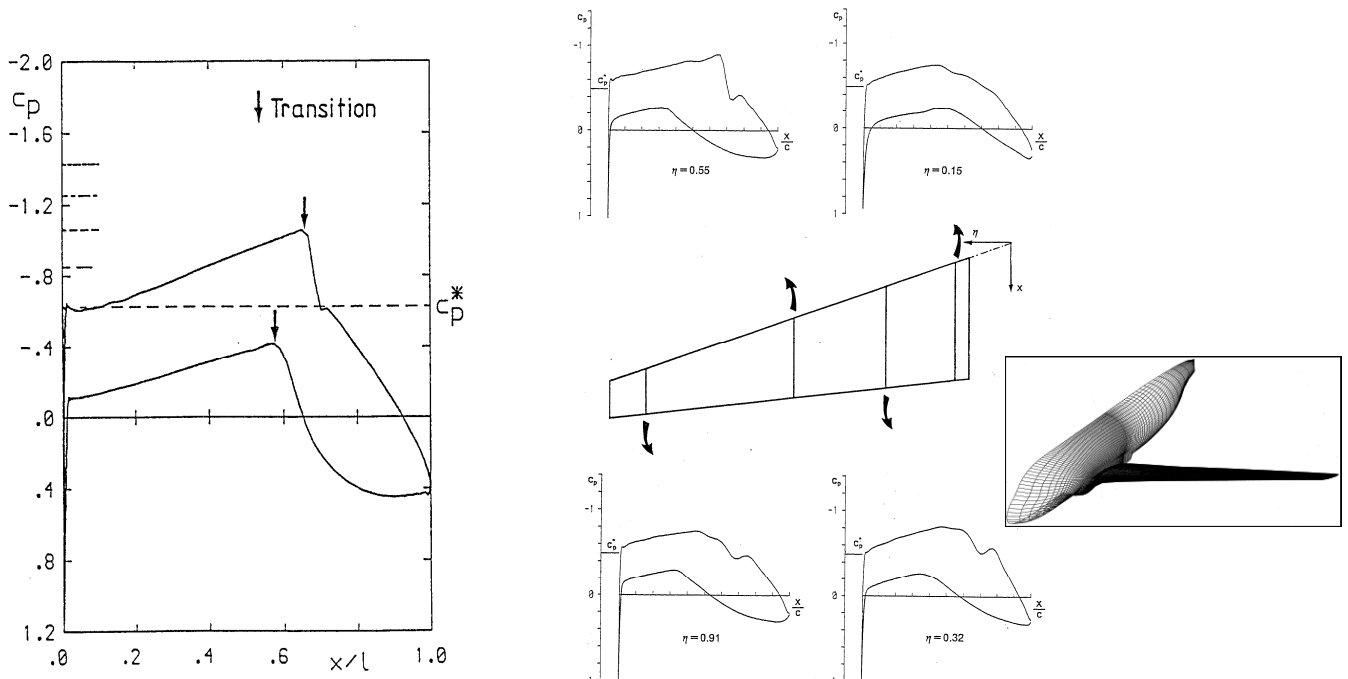


Fig. 2. Typical target pressure distribution

Fig. 3. Pressure distribution on NLF wing at design point

Fig. 4. Spanwise distribution of Re_θ for NLF wing design

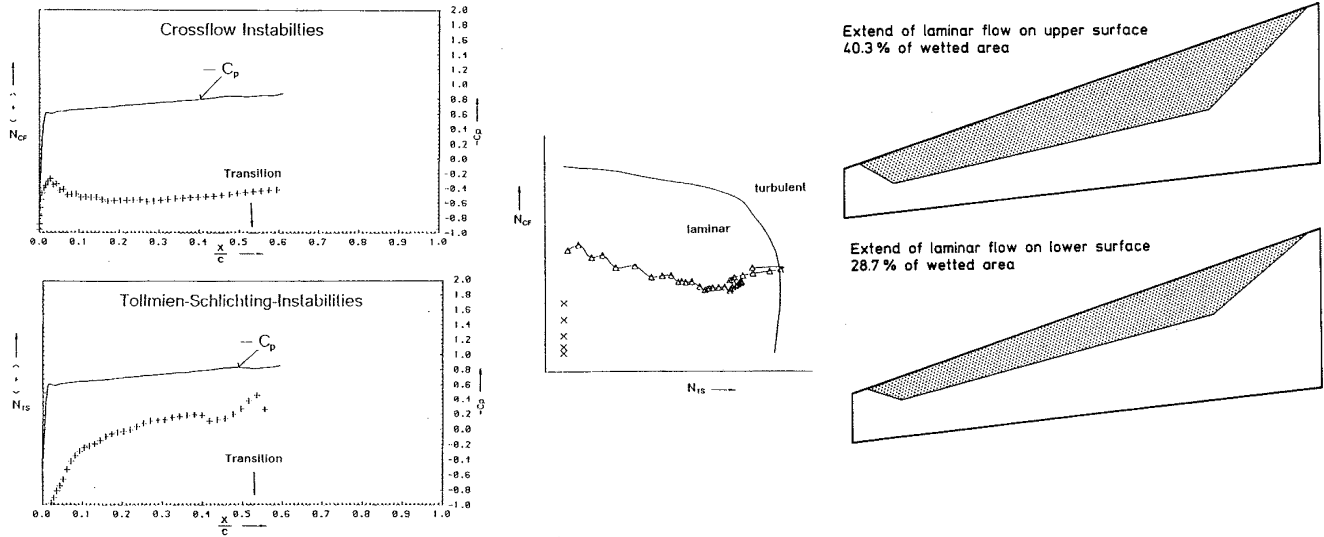
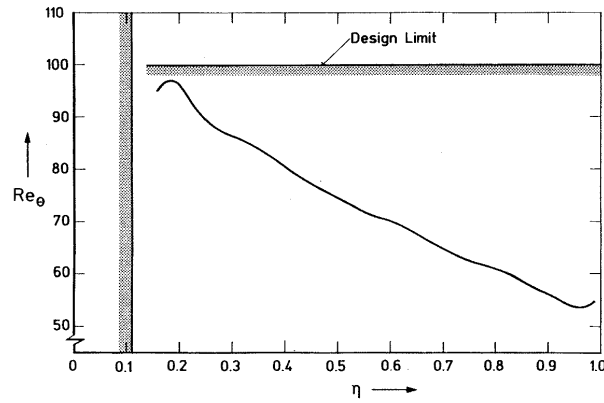


Fig. 5. Transition prediction at span station $\eta = 0.55$, wing upper side, $Re_C = 19.6 * 10^6$ as example

$Ma = .716$, $Re_{AMC} = 11.54 * 10^6$, $C_L = .25$

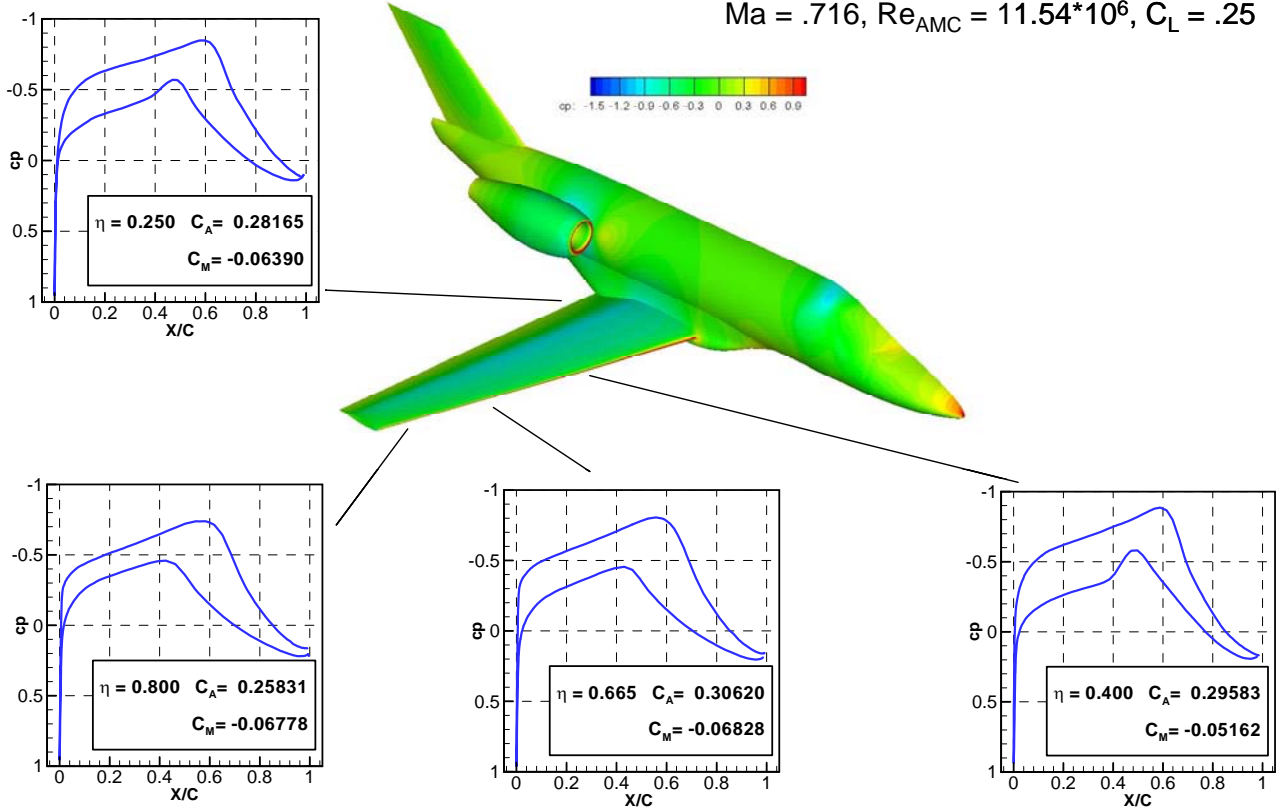


Fig. 6. Pressure distributions on wing of VLJ business aircraft at design point

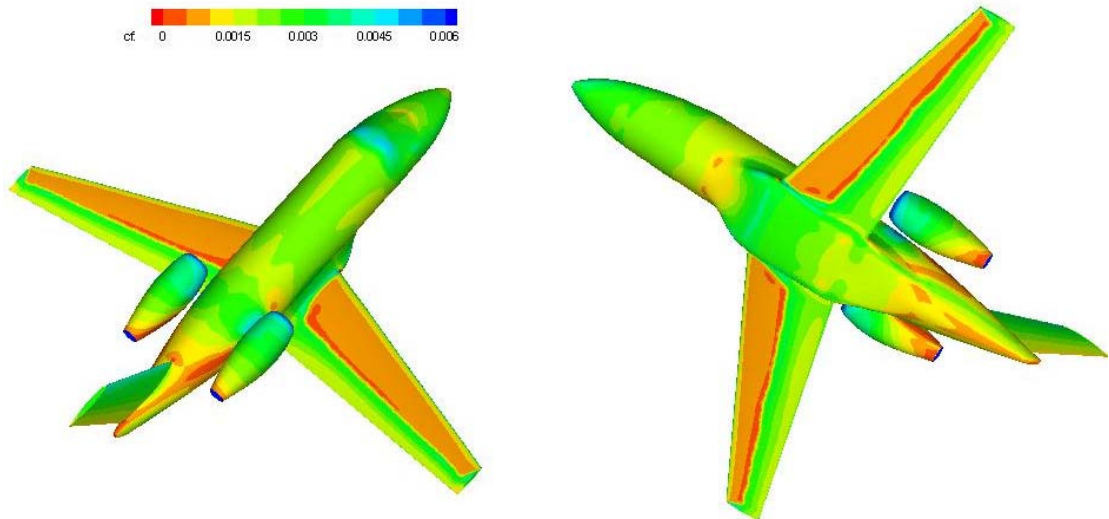


Fig. 7. Local skin friction coefficient on VLJ business aircraft at design point showing laminar areas on wing

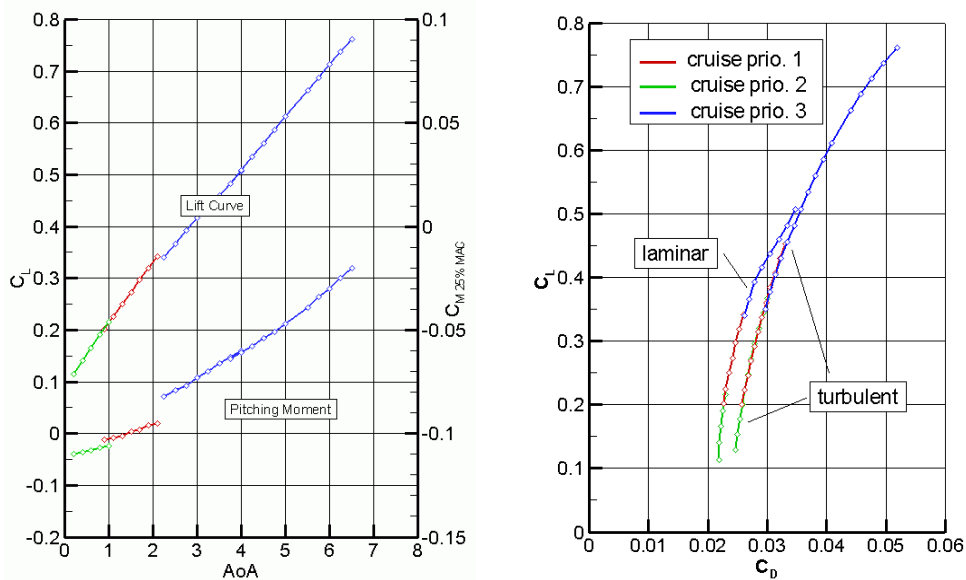


Fig. 8. Lift curve, pitching moment and drag polar for VLJ business aircraft in cruise condition

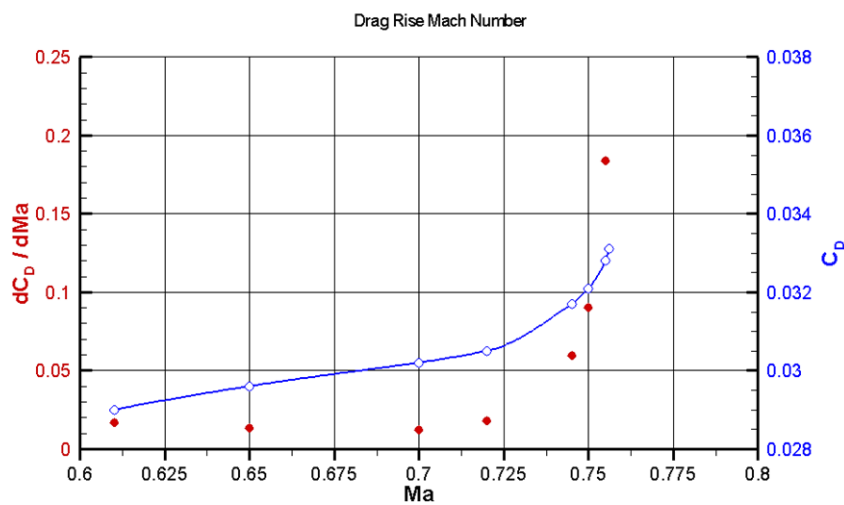


Fig. 9. Evaluation of drag rise; requirement: $dC_D/dMa < 0.1$ at $C_L = 0.34$ and $Ma = 0.75$

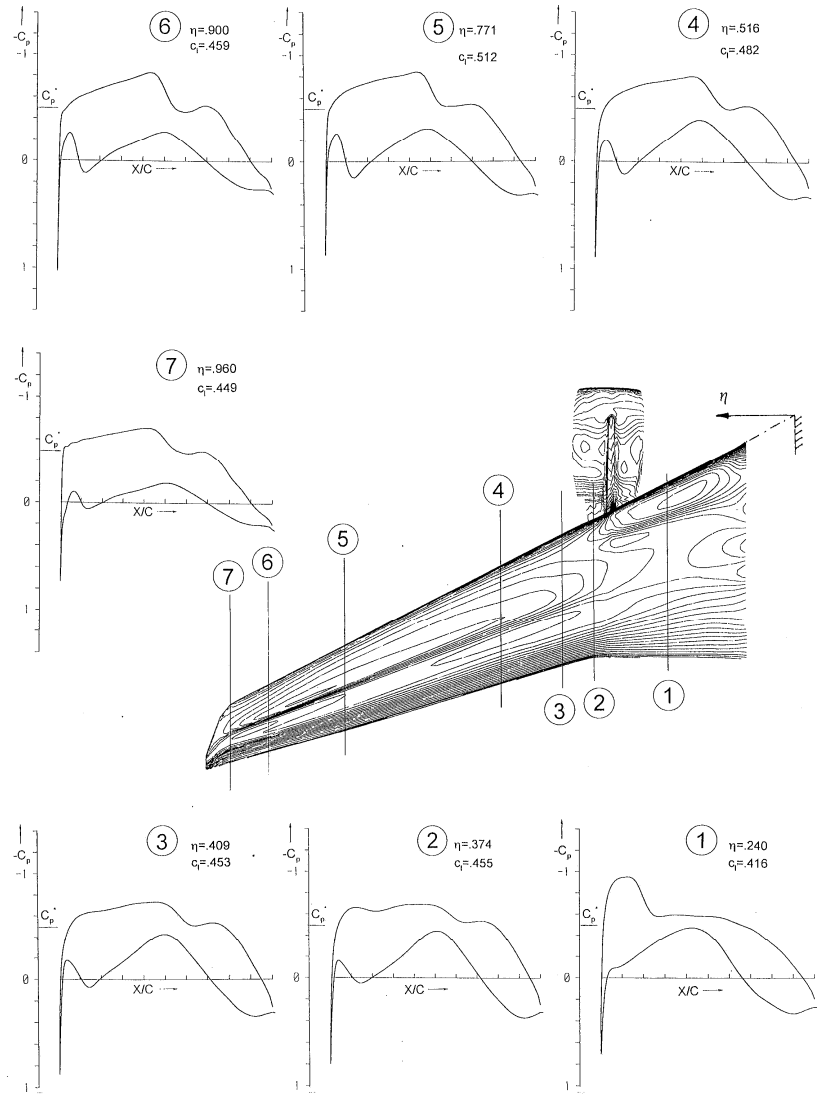


Fig. 10. Pressure distributions on HLFC wing at design point

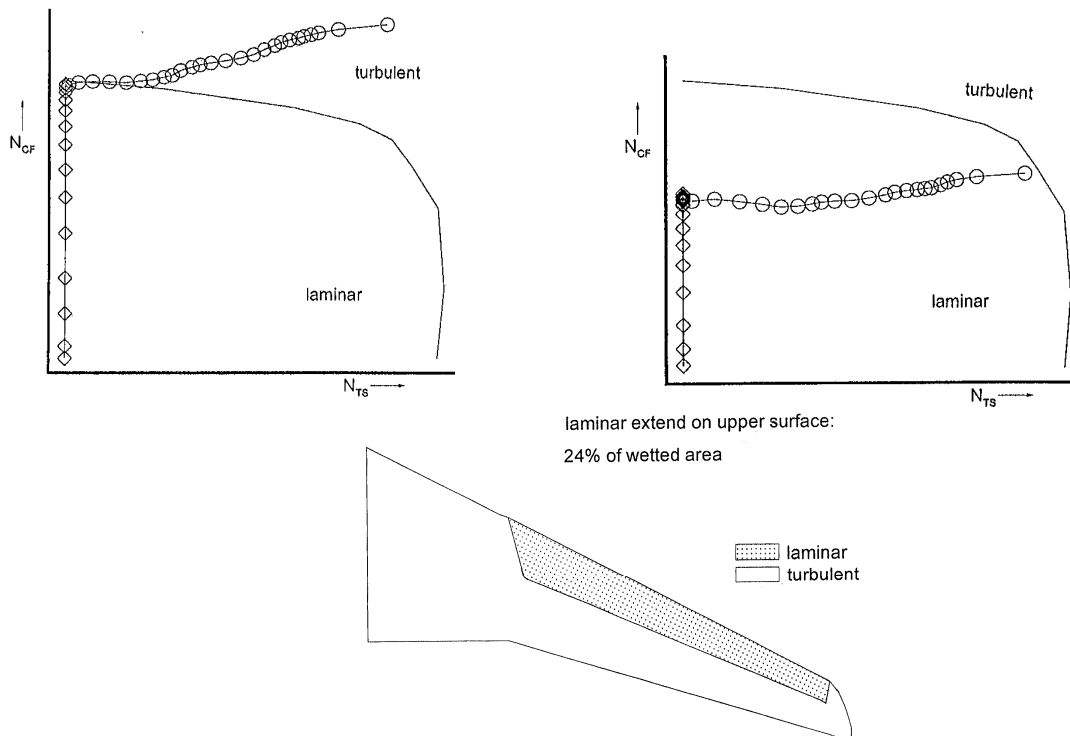


Fig. 11. n_{TS} - n_{CF} diagrams for span station $\eta = 0.516$, with and without suction and laminar wetted area

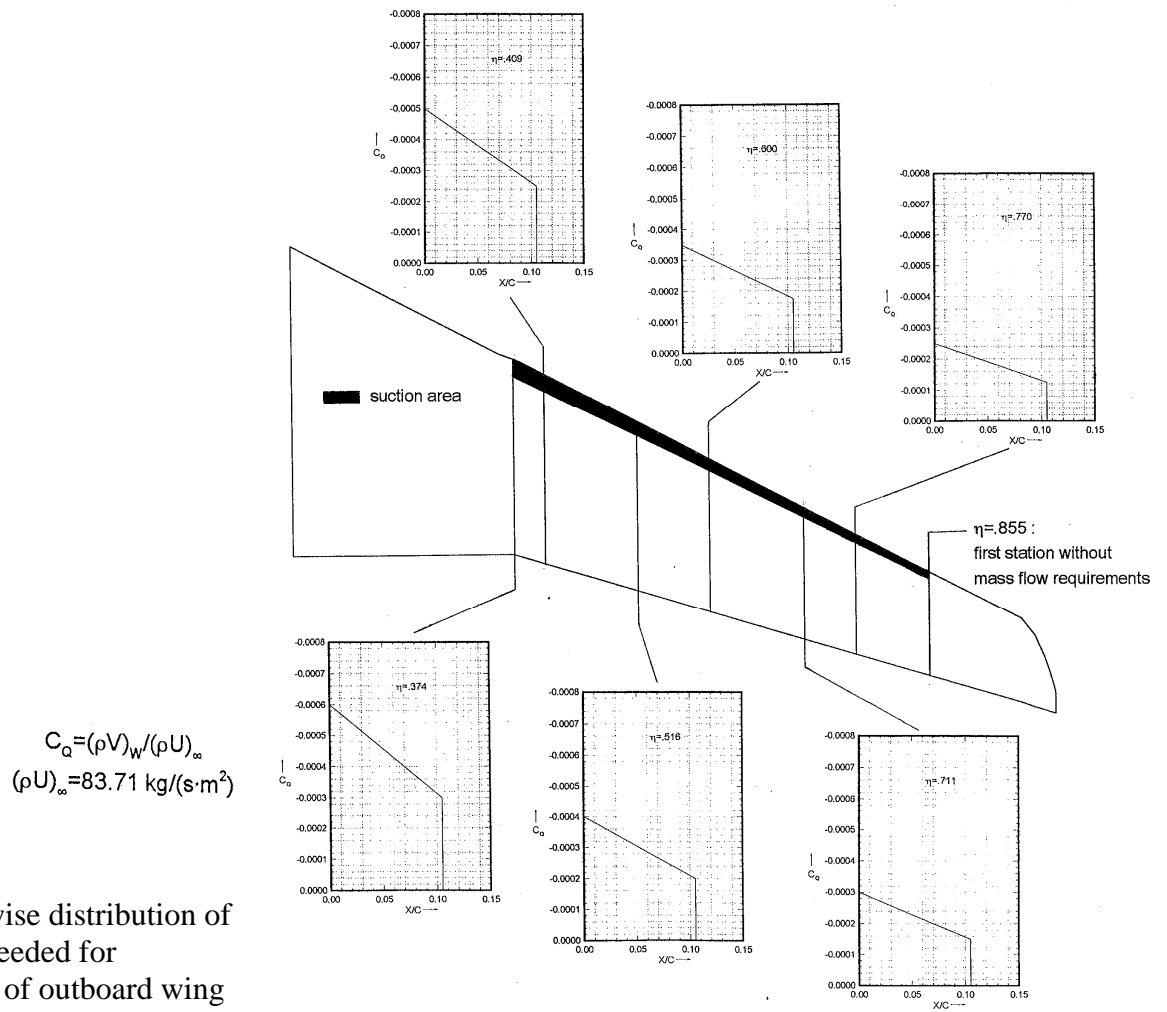


Fig. 12. Spanwise distribution of suction rates needed for laminarization of outboard wing

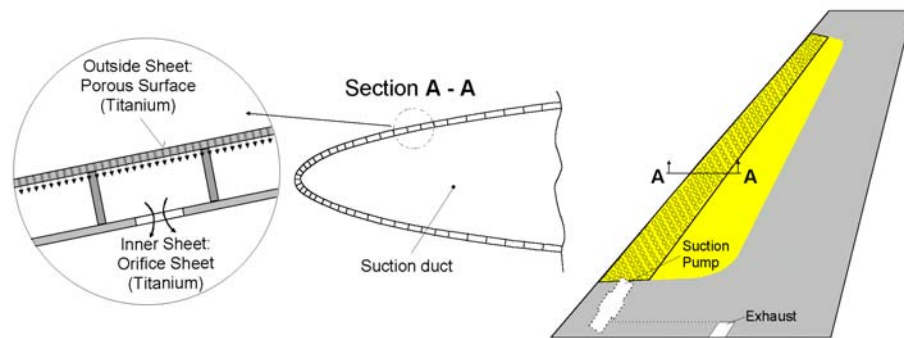


Fig. 13. Principle layout of the ALTTA simplified suction system

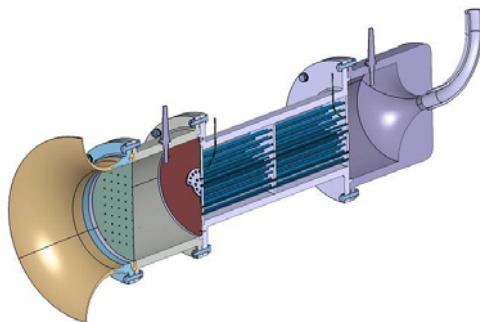


Fig. 14. Flowmeter to measure pressure drop across porous surfaces and metering orifices; measurements are performed in a climate chamber